A Well-Balanced Stochastic Galerkin Method for Scalar Hyperbolic Balance Laws with Random Inputs

Shi Jin, Dongbin Xiu & Xueyu Zhu

Journal of Scientific Computing

ISSN 0885-7474
Volume 67
Number 3

J Sci Comput (2016) 67:1198-1218
DOI 10.1007/s10915-015-0124-2

Springer

J Sci Comput (2016) 67:1198–1218
DOI 10.1007/s10915-015-0124-2

A Well-Balanced Stochastic Galerkin Method for Scalar Hyperbolic Balance Laws with Random Inputs

Shi Jin[1,2] · **Dongbin Xiu**[3] · **Xueyu Zhu**[4]

Received: 4 February 2015 / Revised: 21 September 2015 / Accepted: 17 October 2015 /
Published online: 5 November 2015

Abstract We propose a generalized polynomial chaos based stochastic Galerkin methods for scalar hyperbolic balance laws with random geometric source terms or random initial data. This method is well-balanced (WB), in the sense that it captures the stochastic steady state solution with high order accuracy. The framework of the stochastic WB schemes is presented in details, along with several numerical examples to illustrate their accuracy and effectiveness. The goal of this paper is to show that the stochastic WB scheme yields a more accurate numerical solution at steady state than the non-WB ones.

Keywords Uncertainty quantification · Hyperbolic balance laws · Well-balanced schemes · Generalized polynomial chaos · Stochastic Galerkin

1 Introduction

Hyperbolic systems with geometric source terms arise in various applications, for example, shallow water with bottom tomography, nozzle flows, etc. In these applications, the source terms may have low regularity or concentrations, which often cause numerical difficulties

✉ Dongbin Xiu
dongbin.xiu@utah.edu

Shi Jin
jin@math.wisc.edu

Xueyu Zhu
xzhu@sci.utah.edu

1 Department of Mathematics, University of Wisconsin, Madison, WI 53706, USA

2 Department of Mathematics, Institute of Natural Sciences and MOE-LSC, Shanghai Jiao Tong University, Shanghai 200240, China

3 Scientific Computing and Imagining Institute and Department of Mathematics, University of Utah, Salt Lake City, UT 84112, USA

4 Scientific Computing and Imaging Institute, University of Utah, Salt Lake City, UT 84112, USA

to obtain accurate steady state solutions c.f., [13]. The steady state solutions computed by the standard shock capturing schemes may show notable discrepancy with the true steady state solutions. It is understood that this is due to the inevitable numerical viscosity in the shock capturing schemes. To circumvent the difficulty, *well-balanced* (WB) schemes were developed to capture the steady state solutions either exactly or with at least second order accuracy. Since its first introduction in [14], WB schemes have been under extensive studies, see for examples, [2–4,8,12–16,22,24,25] and references therein.

In practice, uncertainty is ubiquitous and often has non-negligible effects on the simulation results. For example, in shallow-water equations the bottom topography is almost always uncertain [1,7,17]. Uncertainty can also enter the system via initial and boundary conditions. Propagation of uncertainty for these systems has been studied, c.f., [9,18], in conjunction with the standard shock capturing schemes. In [18], a stochastic collocation method based on deterministic WB schemes for the shallow water equations, combined with a multi-level Monte-Carlo method, was used to quantify the uncertainty due to the random bottom topography. Though stochastic Galerkin approaches of hyperbolic conservation laws with random inputs were investigated, c.f., [5,20,23], the development of stochastic Galerkin methods in the context of WB schemes has been, to our best knowledge, non-existent.

In this paper, we present a set of *stochastic WB methods* for scalar hyperbolic conservation laws with random inputs. More specifically, we employ generalized polynomial chaos (gPC) approach expansion [27], combined with stochastic Galerkin (SG) method, in the random space. While the gPC–SG approach has been adopted for a large variety of stochastic problems, this paper represents the first attempt to construct stochastic WB (sWB) schemes. The sWB methods are built upon the idea of the deterministic WB method, via the so-called *interface methods* [15], and are illustrated by two prototype problems with different types of nonlinearity. We will show that the carefully constructed gPC-Galerkin method is WB, in the sense that it becomes a gPC-Galerkin approximation for the steady state equation with at least second order accuracy on a relatively coarse mesh.

While this paper is the first step toward developing stochastic WB Galerkin schemes for nonlinear hyperbolic systems of balance laws, its generalization to nonlinear systems still face the major challenge of the loss of global hyperbolicity [6]. Extra efforts, for example by using the entropy variables, are needed to handle this difficulty. This will be a subject of future study.

The paper is organized as follows. In Sect. 2, we discuss some preliminary materials about the deterministic WB schemes. In Sect. 3, we shall give a formal definition of stochastic WB schemes, and then present the details of the stochastic WB schemes for the two example equations and study their WB properties. Finally in Sect. 4, we provide several numerical examples to illustrate the effectiveness of the sWB methods.

2 Preliminaries

To illustrate the idea of the well-balanced (WB) schemes, let us consider a scalar conservation law with a particular for source term, which serves a model problem for many well-balanced schemes [3]

$$\partial_t u + \partial_x f(u) = -b'(x)q(u), \tag{2.1}$$

where $b(x)$ represents the bottom topography and $q(u)$ is typically related with the drag force. The steady state equation is given by

$$\partial_x f(u) + b'(x)q(u) = 0, \tag{2.2}$$

or, if the solution is smooth,

$$f'(u)\partial_x u + b'(x)q(u) = 0. \tag{2.3}$$

Let

$$D(u) = \int_0^u \frac{f'(u)}{q(u)} ds, \tag{2.4}$$

then (2.3) can be integrated to give the following algebraic expression

$$D(u(z)) + b(x) = \text{constant}. \tag{2.5}$$

Hereafter we will call (2.2) the *steady state equation*, and (2.5) the *steady state condition*.

Due to the first order numerical viscosity used in shock capturing methods, a standard discretization (split or unsplit) over (2.1) fails to preserve the steady state solution (2.5) accurately at the cell average. Rather, a first order numerical discretization error contributes to the numerical discrepancy, especially when the source terms lack regularity [14]. A numerical scheme is called well-balanced (WB) if it can preserve the steady state condition (2.5) either exactly, or formally with at least second order accuracy. Such kind of WB schemes have been well developed for the deterministic problems, see, for examples, [3,4,8,12–16,24,25].

2.1 A Deterministic WB Scheme

To illustrate the idea behind WB schemes, we now briefly review a straightforward deterministic WB scheme proposed in [15]. For smooth solutions, it preserves the steady state condition (2.5) formally with at least second order accuracy at the cell *interfaces*. In this scheme one uses only the solution at the interfaces, which are readily available in the associated upwinding numerical flux (e.g., Godunov or Roe type) for the source term. Subsequently, one can also obtain a formally high order approximation of (2.5) for the cell averages.

Here we adopt the finite volume framework. For spatial discretization, we choose the spatial grids $x_{j+1/2}$, $j = 1, \ldots, N_x$, with a uniform mesh size $\Delta x = x_{j+1/2} - x_{j-1/2}$. The discrete time level t^n are also uniformly spaced with a time step $\Delta t = t^{n+1} - t^n$, where n is the temporal index. The cell average in $[x_{j+1/2}, x_{j-1/2}]$ at time t^n is

$$u_j^n = \frac{1}{\Delta x} \int_{x_{j-1/2}}^{x_{j+1/2}} u(x, t^n) dx.$$

The numerical scheme proposed in [15] for (2.1) takes the following form,

$$\partial_t u_j + \frac{f_{j+1/2} - f_{j-1/2}}{\Delta x} = -\frac{b_{j+1/2} - b_{j-1/2}}{\Delta x} \frac{q_{j+1/2} + q_{j-1/2}}{2}, \tag{2.6}$$

where $q_{j+1/2} = q(u_{j+1/2})$, $b_{j+1/2} = b(x_{j+1/2})$, and $f_{j+1/2}$ is the numerical flux of $f(u)$ at the cell interface $x_{j+1/2}$. Different definitions of the flux yield different shock capturing methods. For example, in the well known Godunov [11] or Roe [21] method, $f_{j+1/2} = f(u_{j+1/2})$, where $u_{j+1/2}$ is the solution of the Riemann or the approximate Riemann problem for $u_t + f(u)_x = 0$ with initial data u_j for $x < 0$ and u_{j+1} for $x > 0$. In (2.6), the right-hand-side is expressed at the cell interfaces. Hereafter we will refer this scheme to the *interface method*. Obviously, it provides a second order discretization of the source term on the right-hand-side. The temporal discretization is by the standard forward Euler method. For steady state solutions, the order of the temporal discretization is not important. Nevertheless, one can use higher-order ODE solvers if higher order accuracy is desired for transient problems. A theoretical study of this method is given in [19].

If $D(u)$ is monotone, the following interface method for (2.1) is more accurate,

$$\partial_t u_j + \frac{f_{j+1/2} - f_{j-1/2}}{\Delta x} = -\frac{b_{j+1/2} - b_{j-1/2}}{\Delta x} \frac{f_{j+1/2} - f_{j-1/2}}{D_{j+1/2} - D_{j-1/2}} \tag{2.7}$$

Clearly, the discretization of the source term is second order.

For the steady state solution, one drops the time derivative in (2.7) and obtains

$$\frac{f_{j+1/2} - f_{j-1/2}}{\Delta x} + \frac{b_{j+1/2} - b_{j-1/2}}{\Delta x} \frac{f_{j+1/2} - f_{j-1/2}}{D_{j+1/2} - D_{j-1/2}} = 0. \tag{2.8}$$

This leads to

$$D_{j+1/2} - D_{j-1/2} + b_{j+1/2} - b_{j-1/2} = 0, \tag{2.9}$$

and subsequently,

$$D_{j+1/2} + b_{j+1/2} \equiv \text{constant}, \qquad \text{for all} \quad j\,. \tag{2.10}$$

Therefore, the correct steady state condition (2.5) is preserved *exactly* at the cell interface $x_{j+1/2}$.

On the other hand, a natural way to discretize (2.1) uses the cell average of u_j in the source term. This is the more conventional method and will be termed as *cell-average method*,

$$\partial_t u_j + \frac{f_{j+1/2} - f_{j-1/2}}{\Delta x} = -\frac{b_{j+1/2} - b_{j-1/2}}{\Delta x} q(u_j)\,. \tag{2.11}$$

Unlike the aforementioned interface method, this method is not WB [15].

3 Stochastic Well-Balanced Schemes

We now extend the deterministic WB schemes into stochastic setting to take into account uncertainty in the underlying problems. To this end, we consider the same problem (2.1) subject to a random source term:

$$\partial_t u + \partial_x f(u) = -b'(x, z)q(u), \tag{3.1}$$

where $z \in I_z \subseteq \mathbb{R}^d, d \geq 1$, is a set of random variables with probability density function $\rho(z)$. These random variables are used to parameterize the uncertainty in the bottom topography function b. (Parameterization of random processes may be a non-trivial task, especially for non-Gaussian processes. This is, however, a topic out of the scope of the current paper. For interested readers, we refer to [26] and the references therein.) We now extend the concept of deterministic WB scheme to stochastic setting.

Definition 3.1 (*stochastic WB*). Let $\mathcal{S}$ be a numerical scheme for (3.1), which results in a solution $v(z) \in V_z$, where V_z is a finite dimensional linear function space. A numerical scheme $\mathcal{S}$ is called strongly well-balanced if it preserves the steady state condition (2.5) either exactly or formally with at least second order accuracy (in physical space) for almost every $z \in I_z$; it is weakly well-balanced if its steady-state solution $v(z)$ satisfies the weak form (in the sense of Galerkin) of Eq. (2.2) formally with at least second order accuracy (in physical space).

Even though this definition is expressed in the context of (3.1), it can be readily applied to other proper systems. It is obvious that the strong WB is difficult to achieve, as it almost requires the analytical solution of (3.1) over the entire random space I_z. On the other hand,

the weak WB is easier to achieve. Notice that here the weak form is imposed on the steady-state Eq. (2.2), instead of (2.5). This is because during the derivation of (2.5), $q(u)$ is divided on both sides of (2.2). Such an operation (division) can only be applied in the strong sense, i.e., for almost every z in I_z. Hence, imposing weak form is natural on (2.2) but not on (2.5). Even for the deterministic WB schemes, whenever the solutions are discontinuous, one only has (2.2) instead of (2.5). Clearly (2.5) implies (2.2) but not vice versa if the solution is not smooth.

Hereafter we will only discuss the weak stochastic well-balanced schemes and refer them to as *stochastic well-balanced (sWB) schemes*. In the following sections we shall derive sWB schemes using the generalized polynomial chaos (gPC) expansion, as examples, for two nonlinear fluxes: $f(u) = u^2/2$ (the inviscid Burgers' equation) and $f(u) = u^4/4$.

3.1 The gPC Approximation and Stochastic Galerkin

We now briefly review the gPC method [10,27] and its Galerkin formulation for general stochastic differential equations with random inputs:

$$\partial_t u = \mathcal{L}(t, x, u, z; b(x, z)), \tag{3.2}$$

where proper initial and boundary conditions are assumed. Again $z \in I_z \subseteq \mathbb{R}^d$, $d \geq 1$ parameterizes the random inputs and $b(x, z)$ represents the bottom topography with a random imput.

In the most common gPC setting, one seeks a numerical solution in term of d-variate orthogonal polynomials of degree $N \geq 1$. That is, the linear space V_z in Definition 3.1 is set to be $\mathbb{P}_N^d$, the space of d-variate orthogonal polynomials of degree up to $N \geq 1$. For fixed x and t, we seek an approximation,

$$u(x, t, z) \approx u_N(x, t, z) = \sum_{m=1}^{M} \hat{u}_m(t, x)\Phi_m(z), \tag{3.3}$$

where $\hat{u}_m$ is the m-th expansion coefficient for $1 \leq m \leq M$ with

$$M = \dim \mathbb{P}_N^d = \binom{d+N}{d}, \tag{3.4}$$

and $\{\Phi_m\} \subset \mathbb{P}_N^d$ are orthonormal polynomials satisfying

$$\int \Phi_i(z)\Phi_j(z)\rho(z)\,dz = \delta_{ij}, \qquad 1 \leq i, j \leq M = \dim\left(\mathbb{P}_N^d\right). \tag{3.5}$$

Here $\rho(z)$ is the probability density function of z and δ_{ij} the Kronecker delta function. Note that when the random dimension $d > 1$, an ordering scheme for multiple index is required to express (3.3) using the single index m. Typically, the graded lexicographic order is used, see, for example, Sect. 5.2 of [26]. Based on the associated random distribution ρ, a corresponding orthogonal polynomial basis can be chosen to achieve faster convergence [27].

Using the same gPC expansion, the random input $b(x, z)$ can also be approximated as

$$b(x, z) \approx b_N(x, z) = \sum_{m=1}^{M} \hat{b}_m(x)\Phi_m(z). \tag{3.6}$$

Note that since $b(x, z)$ is a given input process, the expansion is constructed prior to the computation of the governing equation. The construction of this approximation can be obtained in a variety of ways, e.g., interpolation, discrete projection, etc. (see [26] for an overview).

In the gPC-Galerkin formulation, once an appropriate basis is selected, the gPC approximation u_N (3.3) is then inserted into the governing Eq. (3.2) and a Galerkin projection is applied to ensure the residue error is orthogonal to $\mathbb{P}_N^d$. This results in, for each $m = 1, \ldots, M$,

$$\mathbb{E}\left[\partial_t u_N \Phi_m(z)\right] = \mathbb{E}\left[\mathcal{L}(t, x, u, z)\Phi_m(z)\right]. \tag{3.7}$$

Here $\mathbb{E}[\cdot]$ stands for the expectation operator. For continuous distribution, it is an integral over I_z with respect to the probability density function $\rho(z)$. This then results in a system of deterministic equations for the gPC expansion coefficients $\{\hat{u}_m(t, x)\}_{m=1}^M$, for which one can apply proper spatial and temporal discretizations to solve. In the following sections, we shall derive sWB schemes, based on this gPC-Galerkin formulation, for two representative nonlinear fluxes.

3.2 A Stochastic WB Scheme for the Burgers' Equation

We first consider the Burgers' equation with a source term:

$$\partial_t u + \partial_x \left(\frac{u^2}{2}\right) = -b'(x, z)u. \tag{3.8}$$

Its steady state equation is

$$\partial_x \left(\frac{u^2}{2}\right) + b'(x, z)u = 0, \tag{3.9}$$

If $u \neq 0$ and is smooth, this gives

$$u(x, z) + b(x, z) = u_b, \tag{3.10}$$

where an operation (dividing both sides by u) has been carried out for all z. Therefore, this latter formulation can not be treated in a weak form.

To derive the sWB scheme, we first apply the interface method (2.6)–(3.8). We follow the tradition by using subscript j to denote the solution at the jth node in the physical space. Upon using the first-order upwind scheme in both the flux and the source term, we obtain

$$\partial_t u_j + \frac{u_j^2 - u_{j-1}^2}{2\Delta x} = -\frac{b_j - b_{j-1}}{\Delta x}\frac{u_j + u_{j-1}}{2}, \tag{3.11}$$

where to simplify the notation we have assumed $u > 0$ for all x, t (the method is of course not restricted by this assumption). We now perform the gPC approximation in the random space I_z and conduct the stochastic Galerkin projection, as in (3.7), and obtain

$$\mathbb{E}\left[\left(\frac{\partial}{\partial t}u_{N,j} + \frac{u_{N,j}^2 - u_{Nj-1}^2}{2\Delta x}\right)\Phi_m(z)\right] = -\mathbb{E}\left[\frac{b_{N,j} - b_{N,j-1}}{\Delta x}\frac{u_{N,j} + u_{N,j-1}}{2}\Phi_m(z)\right]. \tag{3.12}$$

Obviously, $u_{N,j}$ and $b_{N,j}$ stand for the Nth degree gPC expansion of u and b, respectively, at the jth node in the physical space. By substituting the gPC expansion (3.3) and (3.6) into (3.12) and letting

$$\hat{\mathbf{u}} = (\hat{u}_1, \ldots, \hat{u}_M)^T, \qquad \hat{\mathbf{b}} = (\hat{b}_1, \ldots, \hat{b}_M)^T, \tag{3.13}$$

be the coefficient vectors, one obtains the following gPC-Galerkin scheme

$$\partial_t \hat{\mathbf{u}}_j + \frac{\mathbf{A}_j\hat{\mathbf{u}}_j - \mathbf{A}_{j-1}\hat{\mathbf{u}}_{j-1}}{2\Delta x} = -\frac{(\mathbf{B}_j - \mathbf{B}_{j-1})(\hat{\mathbf{u}}_j + \hat{\mathbf{u}}_{j-1})}{2\Delta x}, \tag{3.14}$$

where $\mathbf{A}_j = \mathbf{A}(\hat{\mathbf{u}}_j) = (a_{mn,j})_{1\le m,n\le M}$ and $\mathbf{B}_j = \mathbf{B}(\hat{\mathbf{b}}_j) = (b_{mn,j})_{1\le m,n\le M}$ are both $M\times M$ symmetric matrices with entries

$$a_{mn,j} = \mathbb{E}\left[u_{N,j}(z)\Phi_m(z)\Phi_n(z)\right] = \sum_{k=1}^{M}\hat{u}_{k,j}e_{kmn},$$
$$b_{mn,j} = \mathbb{E}\left[b_j(z)\Phi_m(z)\Phi_n(z)\right] = \sum_{k=1}^{M}\hat{b}_{k,j}e_{kmn}, \tag{3.15}$$

where $e_{kmn} = \mathbb{E}[\Phi_k\Phi_m\Phi_n]$. For the temporal discretization, any standard method can be employed. Here the forward Euler method is used, as we are interested in the steady state behavior.

Note that the upwind stencil in (3.11) is based on the assumption that $u > 0$. Likewise, the upwind stencil in (3.12) is chosen under the assumption that $u_N > 0$. Under this assumption, the matrix $\mathbf{A}$ is symmetric and positive definition, see for example [28].

Remark 3.1 The scheme (3.14) is a nonconventional upwind scheme for

$$\partial_t\hat{\mathbf{u}} + \partial_x(\mathbf{A}\hat{\mathbf{u}}) = -\mathbf{B}'(x)\hat{\mathbf{u}}, \tag{3.16}$$

as the upwinding is not applied to the characteristic variables but rather the primitive variables component-wise. Obviously, this is not the optimal upwind scheme. Yet one can still show its (linear) stability. Let us consider the following linear hyperbolic system

$$\partial_t U + C\partial_x U = 0, \qquad U\in\mathbb{R}^M,$$

where C is an $M\times M$ symmetric and positive definite constant matrix that admits diagonalization $T^{-1}CT = \Lambda = \mathrm{diag}(\lambda_1,\ldots,\lambda_M)$. Here Λ is a diagonal matrix with positive entries and T is orthogonal. Let us apply the component-wise upwinding scheme and obtain

$$\frac{U_j^{n+1}-U_j^n}{\Delta t} + C\frac{U_j^n - U_{j-1}^n}{\Delta x} = 0. \tag{3.17}$$

Let $V = T^{-1}U$, then V solves a diagonalized hyperbolic system with characteristic speeds given by the diagonal entries of Λ, and V is given by the conventional upwind scheme

$$V_j^{n+1} = (I - \Delta t\Lambda)V_j^n + \Delta t\Lambda V_{j-1}^n$$

that is stable under the standard CFL condition $\max_{1\le i\le M}\lambda_i\Delta t/\Delta x \le 1$. This implies that $\|T^{-1}U\|_2 = \|U\|_2$ will be bounded by the initial data since T is orthogonal.

3.2.1 The WB Property

To establish the well-balance property, we consider the steady state of the gPC Galerkin scheme (3.14):

$$\frac{\mathbf{A}_j\hat{\mathbf{u}}_j - \mathbf{A}_{j-1}\hat{\mathbf{u}}_{j-1}}{2\Delta x} = -\frac{(\mathbf{B}_j - \mathbf{B}_{j-1})(\hat{\mathbf{u}}_j + \hat{\mathbf{u}}_{j-1})}{2\Delta x}. \tag{3.18}$$

On the other hand, let us consider the steady-state governing Eq. (3.9). Its gPC Galerkin approximation is, for each $m = 1,\ldots,M$,

$$\mathbb{E}\left[\left(\frac{u_N^2}{2}\right)_x\Phi_m\right] = -\mathbb{E}\left[(b_N)_x u_N\Phi_m\right]. \tag{3.19}$$

Upon using the gPC expansion (3.3) and (3.6) and the vector notation for the expansion coefficients (3.13), we obtain

$$\frac{\partial}{\partial x}(\mathbf{Au}) + \mathbf{B}'(x)\mathbf{u} = 0, \tag{3.20}$$

where the entries of the matrices $\mathbf{A}(x) = (a_{mn})$ and $\mathbf{B}(x) = (b_{mn})$ are given in (3.15).

It is obvious that the scheme (3.18), which is the steady state of the scheme (3.14), is a *second*-order approximation to the continuous version of the gPC steady-state system (3.20). Consequently, by Definition 3.1, the numerical scheme (3.14) is sWB.

For comparison, the gPC scheme derived via cell-averaging (2.11) takes the following form,

$$\partial_t \hat{\mathbf{u}}_j + \frac{\mathbf{A}_j\hat{\mathbf{u}}_j - \mathbf{A}_{j-1}\hat{\mathbf{u}}_{j-1}}{2\Delta x} = -\frac{(\mathbf{B}_{j+1/2} - \mathbf{B}_{j-1/2})}{2\Delta x}\hat{\mathbf{u}}_j, \tag{3.21}$$

where the matrices $\mathbf{A}$ and $\mathbf{B}$ are defined in (3.15). This cell-averaged system is not well balanced, similar to its deterministic counterpart (2.11).

3.3 A Stochastic WB Scheme for $f(u) = u^4/4$

We now consider a hyperbolic system with a nonlinear flux $f(u) = u^4/2$. That is, we consider

$$\partial_t u + \partial_x\left(\frac{u^4}{4}\right) = -b'(x,z)u, \tag{3.22}$$

whose steady state solution satisfies

$$\partial_x\left(\frac{u^4}{4}\right) + b'(x,z)u = 0. \tag{3.23}$$

If $u \neq 0$, its strong solution satisfies

$$\frac{u^3(x,z)}{3} + b(x,z) = u_b, \qquad \forall z. \tag{3.24}$$

Again, for notational simplicity let us consider the case of $u > 0$. A corresponding well-balanced scheme, using first order upwind scheme in both the flux and the source term, is

$$\partial_t u_j + \frac{u_j^4 - u_{j-1}^4}{4\Delta x} = -\frac{b_j - b_{j-1}}{\Delta x}\frac{u_j + u_{j-1}}{2}. \tag{3.25}$$

By applying the gPC approximations (3.3) and (3.6) and conducting the Galerkin projection, we obtain, for each $m = 1, \ldots, M$,

$$\mathbb{E}\left[\left(\partial_t u_{N,j} + \frac{(u_{N,j})^4 - (u_{N,j-1})^4}{4\Delta x}\right)\Phi_m(z)\right] \tag{3.26}$$

$$= -\mathbb{E}\left[\left(\frac{b_{N,j} - b_{N,j-1}}{\Delta x}\,\frac{u_{N,j} + u_{N,j-1}}{2}\right)\Phi_m(z)\right], \tag{3.27}$$

or, in the matrix-vector form using (3.13),

$$\partial_t \hat{\mathbf{u}}_j + \frac{\mathbf{S}_j\hat{\mathbf{u}}_j - \mathbf{S}_{j-1}\hat{\mathbf{u}}_{j-1}}{4\Delta x} = -\frac{(\mathbf{B}_j - \mathbf{B}_{j-1})(\hat{\mathbf{u}}_j + \hat{\mathbf{u}}_{j-1})}{2\Delta x}, \tag{3.28}$$

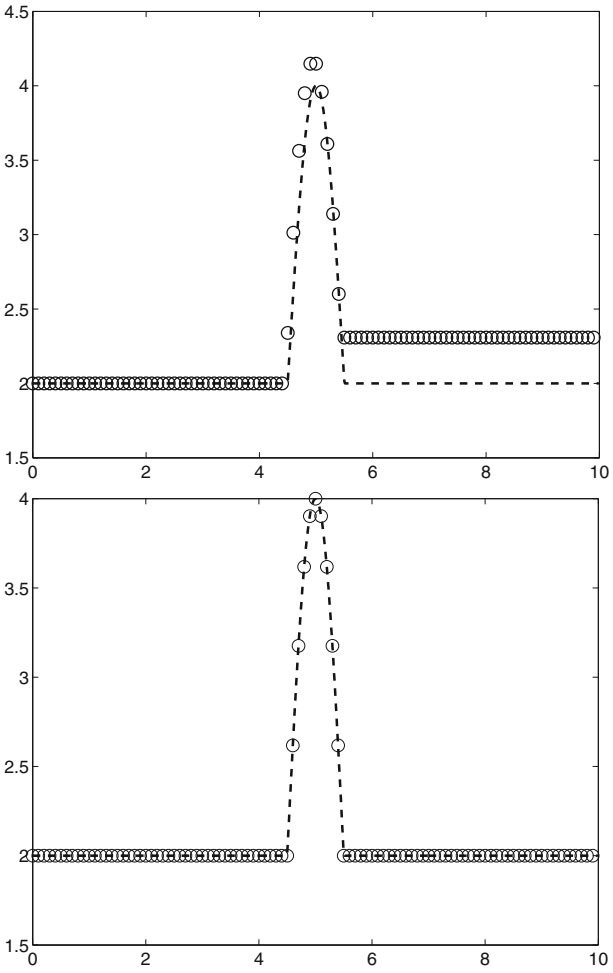

Fig. 1 Burgers' equation with continuous bottom (4.3). Comparison of the mean of u obtained by the 4-th order gPC–SG based on the cell average method (*top*) and the interface method (*bottom*) at the steady state. *Circles* numerical solutions; *dashed lines* exact solution

where $\mathbf{S}_j = \mathbf{S}(\hat{\mathbf{u}}_j) = (s_{mn,j})$ is a $(M \times M)$ matrix with entries

$$s_{mn,j} = \mathbb{E}\left[u_{N,j}^3 \Phi_m \Phi_n\right], \qquad 1 \le m, n \le M.$$

3.3.1 The WB Property

For the well-balanced property, we consider the steady state of the scheme (3.28),

$$\frac{\mathbf{S}_j \hat{\mathbf{u}}_j - \mathbf{S}_{j-1}\hat{\mathbf{u}}_{j-1}}{4\Delta x} = -\frac{(\mathbf{B}_j - \mathbf{B}_{j-1})(\hat{\mathbf{u}}_j + \hat{\mathbf{u}}_{j-1})}{2\Delta x}. \tag{3.29}$$

On the other hand, the steady-state governing Eq. (3.23) leads to the following gPC Galerkin system

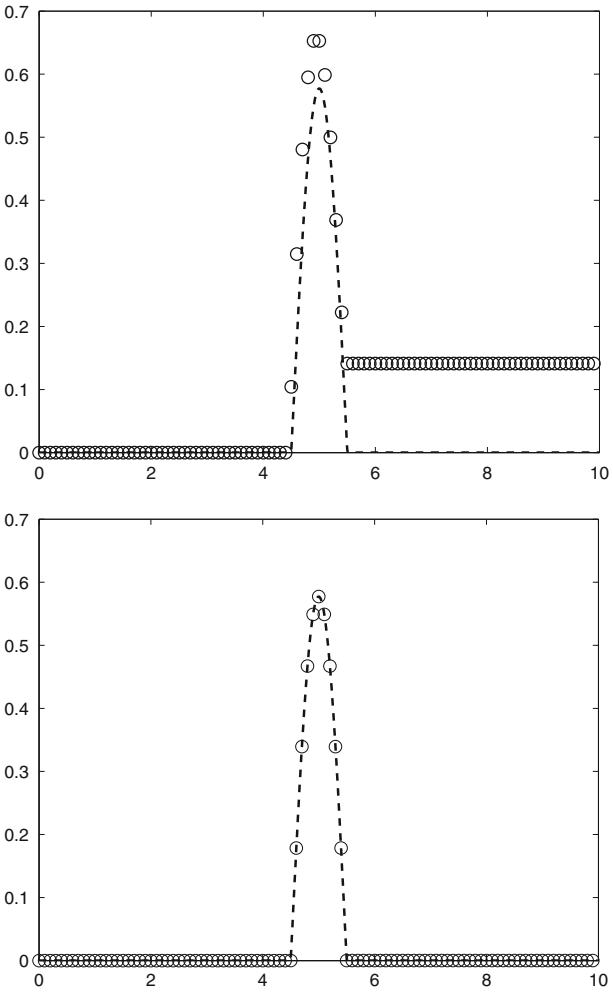

Fig. 2 Burgers' equation with continuous bottom (4.3). Comparison of the standard deviation of u obtained by the 4-th order gPC–SG based on the cell average method (*top*) and the interface method (*bottom*) at the steady state. *Circles* numerical solutions; *dashed lines* exact solution

$$\frac{1}{4}\partial_x\left(\mathbf{S}\hat{\mathbf{u}}\right) + \mathbf{B}'(x)\hat{\mathbf{u}} = 0, \tag{3.30}$$

where the matrix $\mathbf{S} = (s_{mn})_{1\le m,n\le M}$ has entries

$$s_{mn} = \mathbb{E}\left[u_N^3(z)\Phi_m(z)\Phi_n(z)\right], \tag{3.31}$$

and $\mathbf{B}$ is defined in (3.15).

It is then obvious that the steady-state scheme (3.29) is a second-order approximation to the continuous gPC steady state Eq. (3.30). Therefore, the scheme (3.28) is sWB.

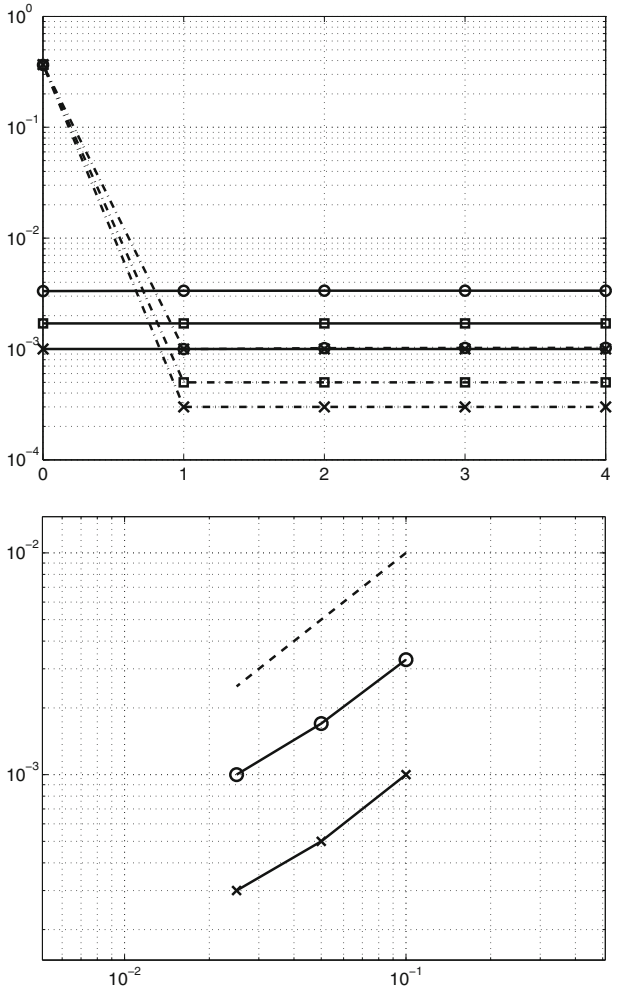

Fig. 3 Burgers' equation with continuous bottom (4.3). Error convergence (*top*) in mean (*solid lines*) and standard deviation (*dashed lines*), with respect to gPC order for $\Delta t = 0.025/8$ (*circles* $\Delta x = 0.1$; *squares* $\Delta x = 0.05$; *crosses* $\Delta x = 0.025$); Error convergence (*bottom*) in mean (*circles*) and standard deviation (*crosses*) obtained by 4-th order gPC–SG method with $\Delta x = 0.1, 0.05, 0.025$, $\Delta t = 0.025/8$, where the *dashline* is the reference line with slope 1

4 Numerical Examples

In this section, we present several numerical examples to demonstrate the effectiveness of the sWB methods. Two error metrics are used: the errors in mean and in standard deviation with l^1 norm in the spatial domain,

$$e_{mean} = \|\mathbb{E}[u^h] - \mathbb{E}[u]\|_{l^1}, \quad e_{std} = \|\sigma_{u^h} - \sigma_u\|_{l^1}, \tag{4.1}$$

where u^h, u are the numerical solution and the reference solution, respectively. The reference mean and standard deviation, if not available in analytical form, are typically computed by high-order stochastic collocation methods, using either tensor Gauss quadrature or sparse

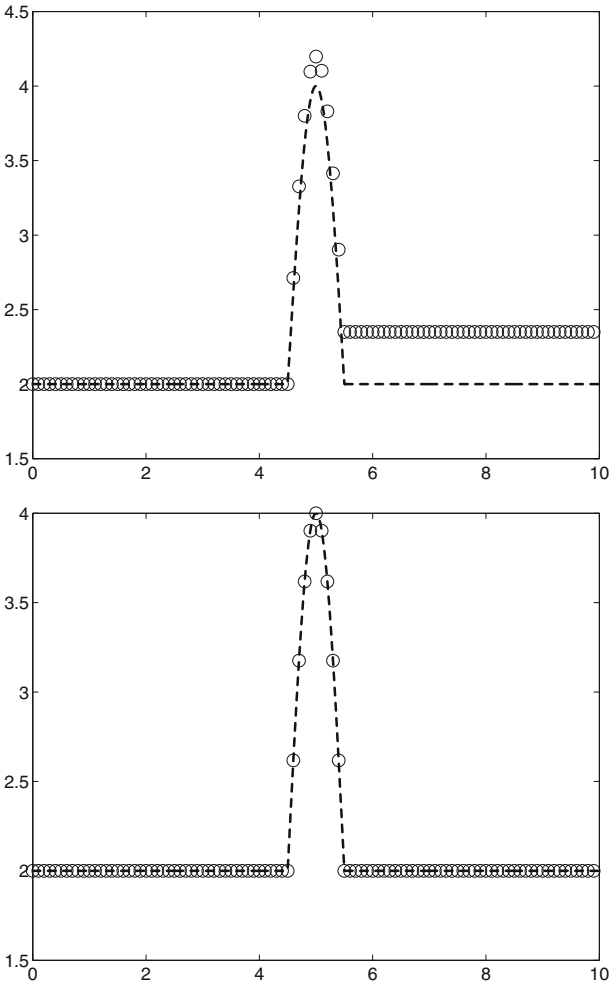

Fig. 4 Burgers' equation with multi-dimensional bottom function given by (4.5) with $\sigma = 1, d = 3$. Comparison of the mean of u obtained by the 4-th order gPC–SG based on the cell average method (*top*) and the interface method (*bottom*) at the steady state. *Circles* numerical solutions; *dashed lines* exact solution

grids quadrature with sufficiently large number of points. We present mostly the cases of univariate random inputs and only a few cases of multi-dimensional random inputs. This makes a thorough examination of the errors straightforward. Applying gPC Galerkin methods to multi-dimensional random inputs represents a rather trivial extension from one-dimension, and has been demonstrated by numerous examples in the literature. We do caution that in high dimensions the computational cost grows fast (curse-of-dimensionality).

4.1 The Burgers' Equation

We first use the Burgers' Eq. (3.8) with the following initial and boundary condition:

$$u(x,0) = 0 \quad \text{for} \quad x > 0\,, \qquad u(0,t) = 2 \quad \text{for} \quad t > 0\,. \tag{4.2}$$

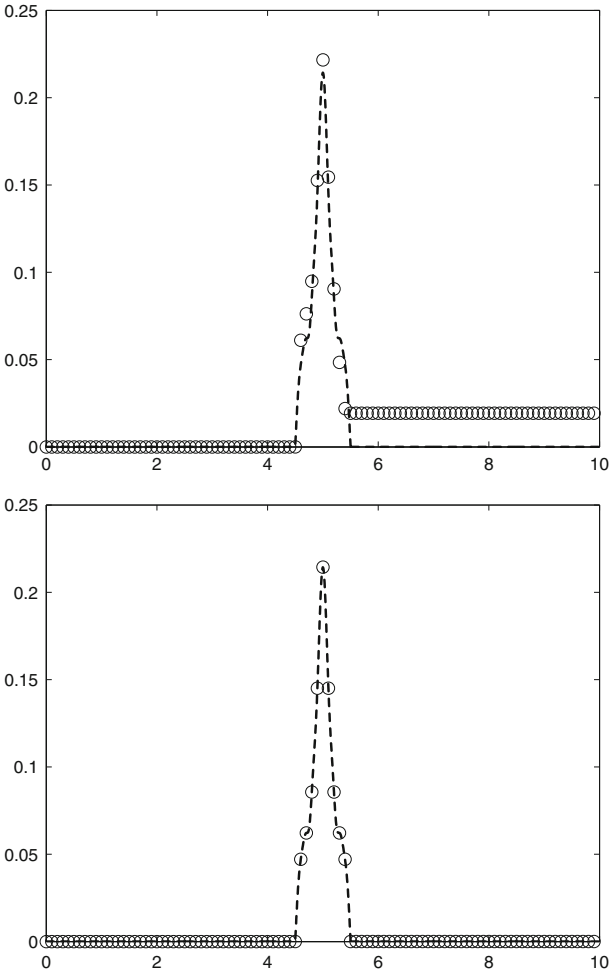

Fig. 5 Burgers' equation with multi-dimensional bottom function given by (4.5) with $\sigma = 1, d = 3$. Comparison of the standard deviation of u obtained by the 4-th order gPC–SG based on the cell average method (*top*) and the interface method (*bottom*) with at the steady state. *Circles* numerical solutions; *dashed lines* exact solution

For a continuous bottom function, $b(x, z)$ is chosen as

$$b(x,z) = \begin{cases} (2+z)\cos(\pi x), & 4.5 \le x \le 5.5; \\ 0, & \text{otherwise.} \end{cases} \tag{4.3}$$

For a discontinuous bottom function, $b(x, z)$ is chosen as

$$b(x,z) = \begin{cases} 0.1(2+z)\cos(\pi x), & 5 \le x \le 6; \\ 0, & \text{otherwise.} \end{cases} \tag{4.4}$$

In all examples, z is a random variable uniformly distributed in $[-1, 1]$.

The spatial discretization is conducted using 100 uniform grid points, and the time step is set to be $\Delta t = 0.025/8$. For the continuous bottom case, the steady state condition is $u = 2 - b$, from which the exact mean and standard deviation can be computed. The

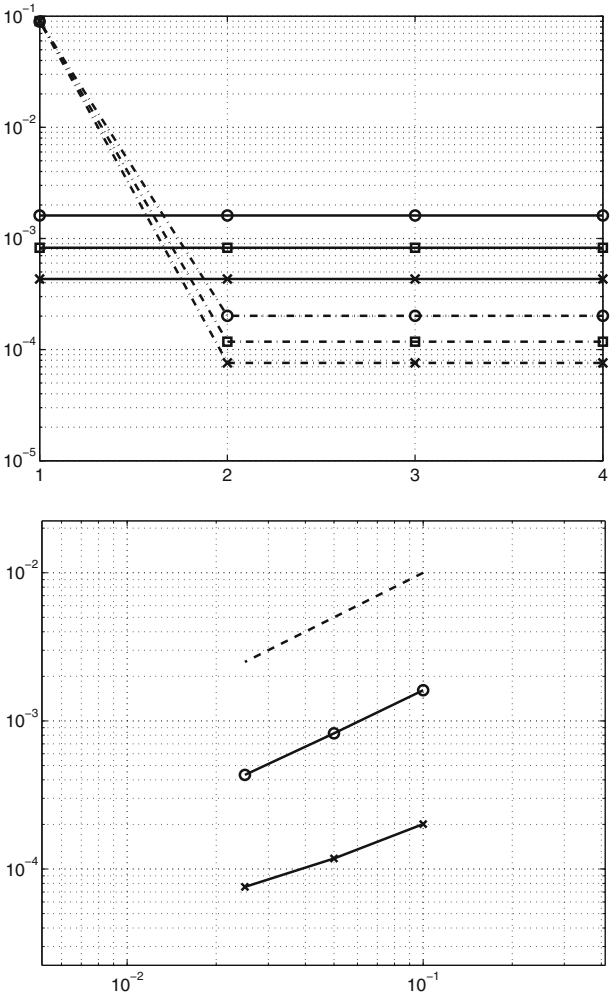

Fig. 6 Burgers' equation with multi-dimensional bottom function given by (4.5) with $\sigma = 1, d = 3$. Error convergence (*top*) in mean (*solid lines*) and standard deviation (*dashed lines*), with respect to gPC order for $\Delta t = 0.025/8$ (*circles* $\Delta x = 0.1$; *squares* $\Delta x = 0.05$; *crosses* $\Delta x = 0.025$); Error convergence (*bottom*) in mean (*circles*) and standard deviation (*crosses*) obtained by 4th order gPC–SG method with $\Delta x = 0.1, 0.05, 0.025$, $\Delta t = 0.025/8$, where the dashline is the reference line with slope 1

numerical results are obtained by the fourth-order ($N = 4$) gPC Galerkin methods, using both the interface scheme (3.14), which is sWB, and the cell-average scheme (3.21), which is not sWB. The comparisons are shown in Figs. 1 and 2, for the mean and the standard deviation, respectively. The difference is notable—the interface scheme (3.14) is sWB and able to capture the steady state satisfactorily; the cell-average scheme (3.21) is not sWB and leads to large error behind the bump in the bottom.

The errors based on the interface method at the steady state with respect to increasing gPC order are plotted in Fig. 3, at various levels of grid resolutions, $\Delta x = 0.1$ (circles), $\Delta x = 0.05$ (squares), and $\Delta x = 0.025$ (crosses). The fast exponential convergence with respect to the order of gPC expansion can be observed. The errors quickly saturate at modest gPC orders and the saturation levels become smaller with finer Δx, indicating that the spatial

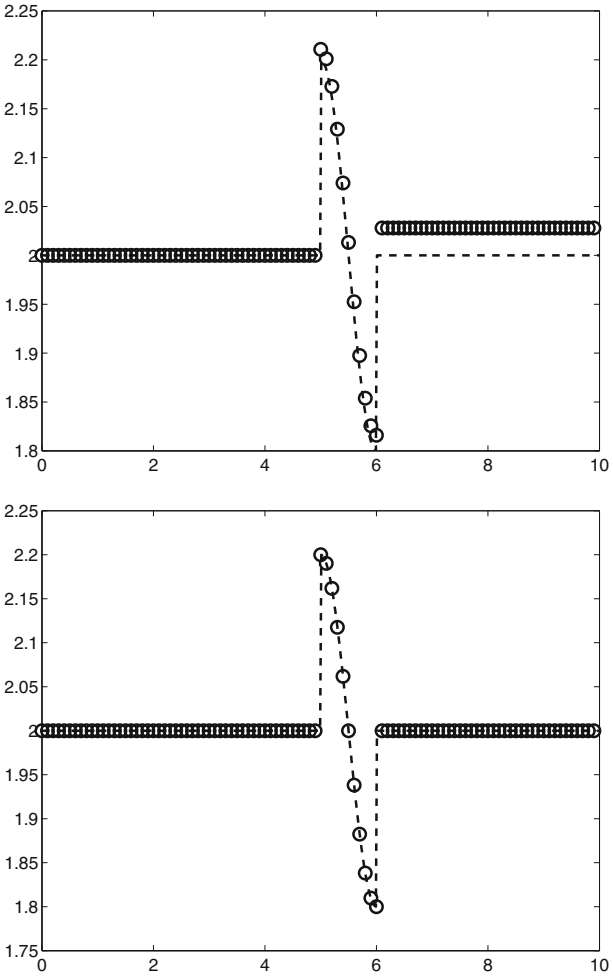

Fig. 7 Burgers' equation with discontinuous bottom (4.4). Comparison of the mean of u obtained by the 5-th order gPC–SG based on the cell average method (*top*) and the interface method (*bottom*) at the steady state. *Circles* numerical solutions; *dashed lines* exact solution

discretization errors are dominant at this stage. In addition, first order convergence in space is clearly observed in l^1 norm for the interface method based on 4-th order gPC–SG method shown in Fig. 3.

We now consider a multi-dimensional random input case, where the bottom function is a random field in the following form,

$$b(x,z) = \begin{cases} \left[2 + \sigma \sum_{i=1}^{d} \frac{1}{i\pi} \cos(2\pi i x) z_i\right] \cos(\pi x), & 4.5 \le x \le 5.5; \\ 0, & \text{otherwise.} \end{cases} \tag{4.5}$$

The formulation for the bump resembles the form of the well known Karhunen-Loeve expansion, widely used for modeling random fields. For benchmarking purpose, we set $\sigma = 1, d = 3$. The mean and standard deviation of the solution are shown in Figs. 4 and 5, where we observe good agreement between the interface scheme based on the 4th

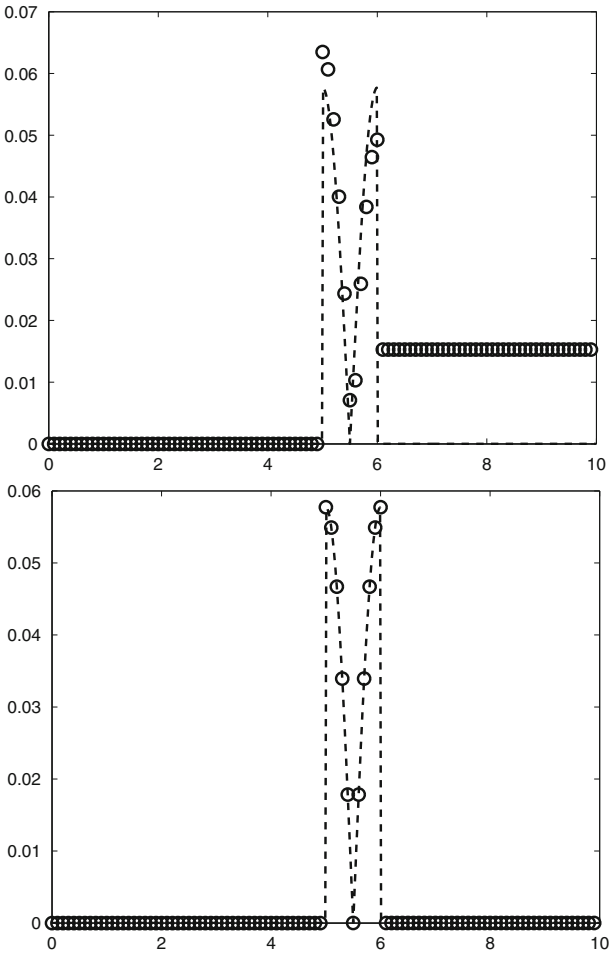

Fig. 8 Burgers' equation with discontinuous bottom (4.4). Comparison of the standard deviation of u obtained by the 5-th order gPC–SG based on the cell average method (*top*) and the interface method (*bottom*) with at the steady state. *Circles* numerical solutions; *dashed lines* exact solution

order gPC-Galerkin method (which is sWB) using 100 uniform grid points and the time step $\Delta t = 0.025/8$, and the reference solutions obtained over 8^d tensor Legendre-Gauss quadrature points. In addition, large error is clearly observed for the cell-average scheme (which is not sWB).

The errors based on the interface method at the steady state with respect to increasing gPC order are plotted in Fig. 6, at various levels of grid resolutions, $\Delta x = 0.1$ (circles), $\Delta x = 0.05$ (squares), and $\Delta x = 0.025$ (crosses). The fast exponential convergence with respect to the order of gPC expansion can be observed. The errors quickly saturate at modest gPC orders and the saturation levels become smaller with finer Δx, indicating that the spatial discretization errors are dominant at this stage. In addition, first order convergence in space is clearly observed in l^1 norm for the interface method based on 4th order gPC–SG method shown in Fig. 6.

The results of the discontinuous bottom case (4.4) are presented in Fig. 7, for the comparison of the mean solution, and in Fig. 8, for the comparison of the standard deviation. Again

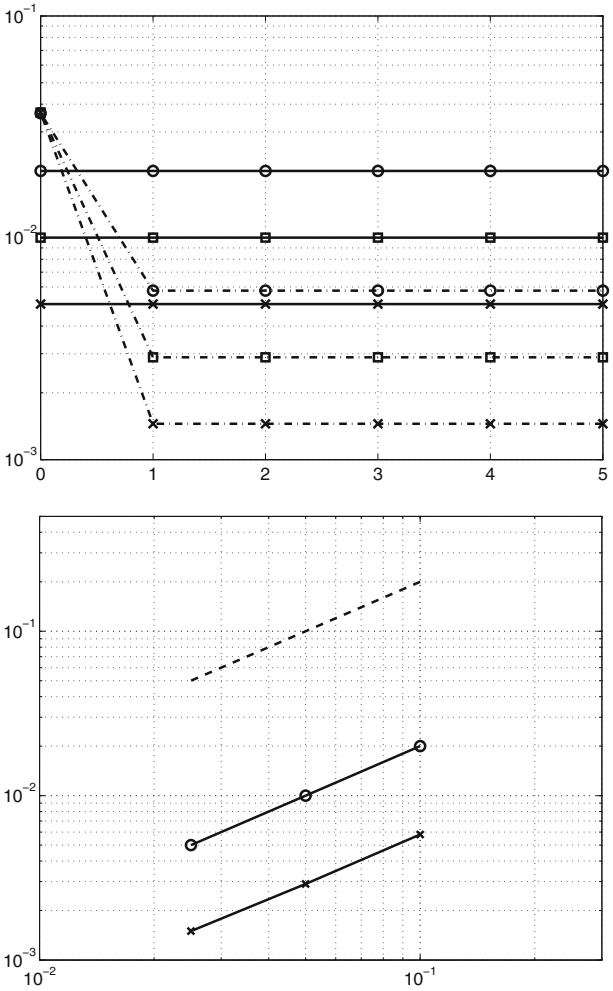

Fig. 9 Burgers' equation with discontinuous bottom (4.4). Error convergence (*top*) in mean (*solid lines*) and standard deviation (*dashed lines*), with respect to gPC order for $\Delta t = 0.025/8$ (*circles* $\Delta x = 0.1$; *squares* $\Delta x = 0.05$; *crosses* $\Delta x = 0.025$); Error convergence (*bottom*) in mean (*circles*) and standard deviation (*crosses*) obtained by 5-th order gPC–SG method with $\Delta x = 0.1, 0.05, 0.025$, $\Delta t = 0.025/16$, where the *dashline* is the reference line with slope 1

the gPC scheme using interface method (3.14) possesses the sWB property and gives much more accurate results than those obtained by the cell-average scheme (3.21), which is not sWB.

The errors based on the interface method at the steady state with respect to increasing gPC order are plotted in Fig. 9, at various levels of grid resolutions, $\Delta x = 0.1$ (circles), $\Delta x = 0.05$ (squares), and $\Delta x = 0.025$ (crosses). The time step is $\Delta t = 0.025/16$. The fast exponential convergence with respect to the order of gPC expansion can be observed. The errors quickly saturate at modest gPC orders and the saturation levels become smaller with finer Δx, indicating that the spatial discretization error is dominant at this stage. In addition, first order convergence in space is clearly observed in l^1 norm for the interface method based on 5-th order gPC–SG method shown in Fig. 9.

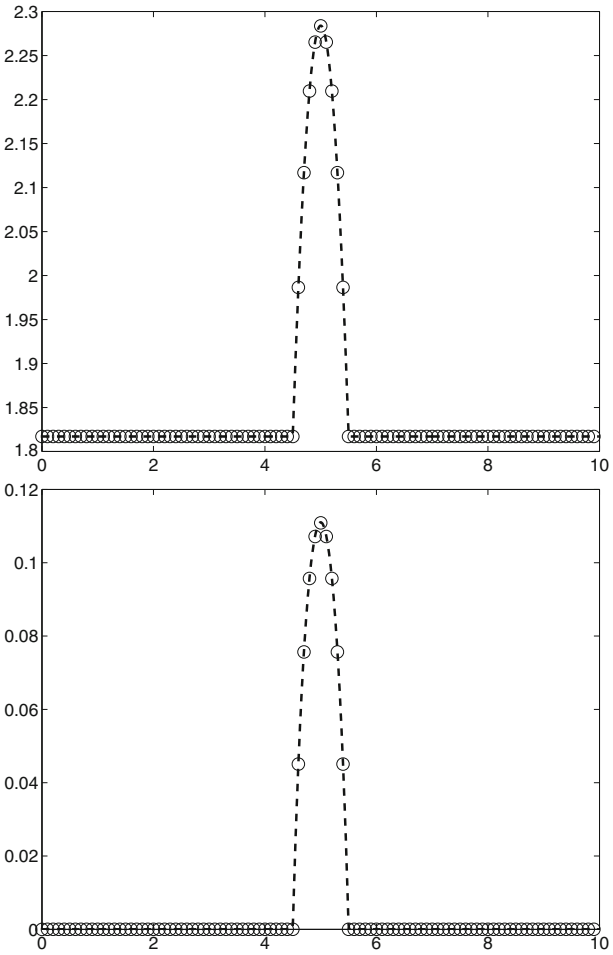

Fig. 10 $f(u) = u^4/4$ with continuous bottom (4.3). Comparison of the mean (*top*) and standard deviation (*bottom*) of u obtained by the 4-th gPC–SG method based on the interface method (*circles*) and the reference solution (*dashed lines*) at the steady state

4.2 The Example with $f(u) = u^4/4$

We now consider the case of $f(u) = u^4/4$, which is discussed in Sect. 3.3. The same continuous bottom function (4.3) as in the previous section is used here. The initial and boundary conditions are

$$u(x, 0) = 0, \quad \text{for} \quad x > 0; \qquad u(0, t) = 6^{\frac{1}{3}}, \quad \text{for} \quad t > 0. \tag{4.6}$$

We use 100 uniformly distributed grid points in space and time step $\Delta t = 0.025/64$. For the continuous bottom, the exact steady state is available, $u = (3(2 - b))^{1/3}$. The numerical results obtained by the fourth order ($N = 4$) interface gPC scheme (3.28), which is sWB, are plotted in Fig. 10. Good agreement can be observed between the gPC–SG solutions and the reference solutions. The numerical errors are plotted in Fig. 11, at various levels of grid

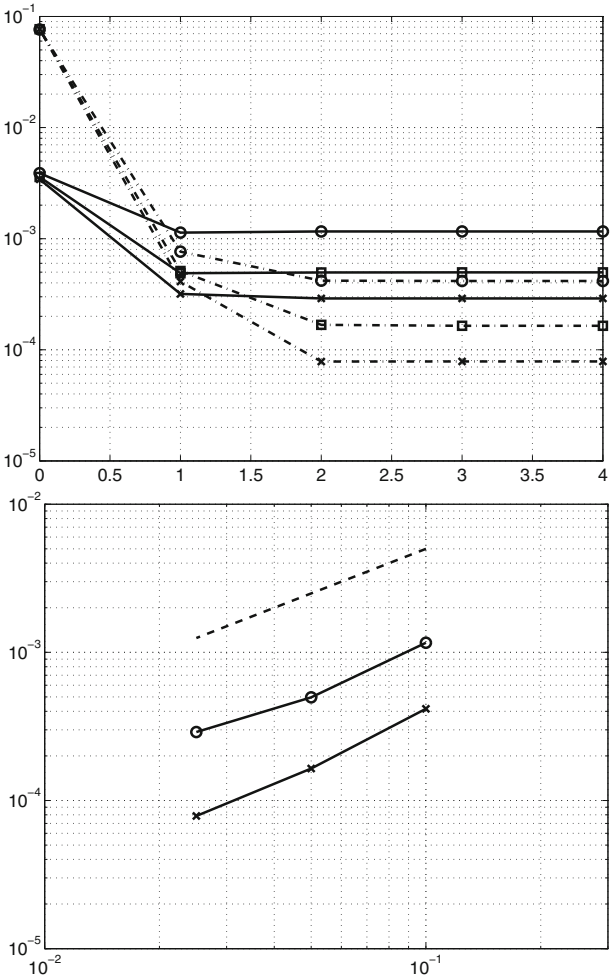

Fig. 11 $f(u) = u^4/4$ with continuous bottom (4.3). Error convergence (*top*) in mean (*solid lines*) and standard deviation (*dashed lines*), with respect to gPC order for $\Delta t = 0.025/8$ (*circles* $\Delta x = 0.1$; *squares* $\Delta x = 0.05$; *crosses* $\Delta x = 0.025$); Error convergence (*bottom*) in mean (*circles*) and standard deviation (*crosses*) obtained by 4-th order gPC–SG method with $\Delta x = 0.1, 0.05, 0.025$, $\Delta t = 0.025/64$, where the *dashline* is the reference line with slope 1

resolutions, $\Delta x = 0.1$ (circles), $\Delta x = 0.05$ (squares), and $\Delta x = 0.025$ (crosses). The time step is $\Delta t = 0.025/64$. The fast exponential convergence with respect to the order of the gPC expansion can be observed. The errors quickly saturate at modest gPC orders, and the saturation levels become smaller with finer Δx. First order convergence is clearly observed in l^1 norm for interface method based on 4-th order gPC–SG method shown in Fig. 11.

5 Summary

In this paper, we proposed a class of stochastic well-balanced (sWB) schemes for scalar hyperbolic conservation laws with random source terms. The new schemes are extensions of

the deterministic WB schemes. They employ the generalized polynomial chaos (gPC) expansion, combined with the stochastic Galerkin projection. We showed that the new schemes are WB in the stochastic setting and demonstrated numerically that they perform better than the not well-balanced ones.

It is worthwhile to remark on the use of stochastic Galerkin and stochastic collocation methods. The gPC Galerkin schemes developed here can enforce the sWB in the entire random space in a weak form, regardless of the order of the gPC approximation. A stochastic collocation method can naturally enforce WB property at the collocation nodes, provided a deterministic WB scheme is employed. It can not, however, guarantee the stochastic WB property at any other locations of the random space. In fact, at lower expansion orders, it can almost surely destroy the WB property away from the collocation nodes because of the approximation errors in the random space. (On the other hand, if one is only interested in the solution statistics, e.g., mean, variance, etc. then stochastic collocation is easier to implement and may be preferred in practice.) This paper serves as the first attempt to develop WB schemes in stochastic Galerkin setting, and we intend to study more for nonlinear systems of hyperbolic balance laws, and higher order numerical fluxes, in the future.

Acknowledgments S. Jin was partially supported by NSF DMS Grants Nos. 1107291 and 1107291: RNMS "KI-Net", and National Science Foundation of China Grant No. 91330203. D. Xiu was partially supported by AFOSR and DOE.

References

1. Bates, P., Lane, S., Ferguson, R.: Parametrization, validation and uncertainty analysis of CFD models of fluvial and flood hydraulics in natural enviroments. In: Computational Fluid Dynamics: Applications in Environmental Hydraulics. Wiley (2005)
2. Bermudez, A., Vazquez, M.E.: Upwind methods for hyperbolic conservation laws with source terms. Comput. Fluids **23**(8), 1049–1071 (1994)
3. Botchorishvili, R., Perthame, B., Vasseur, A.: Equilibrium schemes for scalar conservation laws with stiff sources. Math. Comput. **72**(241), 131–157 (2003)
4. Bouchut, F.: Nonlinear stability of finite volume methods for hyperbolic conservation laws and well-balanced schemes for sources. In: Frontiers in Mathematics. Birkhäuser Verlag, Basel (2004)
5. Bürger, R., Kröker, I., Rohde, C.: A hybrid stochastic galerkin method for uncertainty quantification applied to a conservation law modelling a clarifier-thickener unit. Z. Angew. Math. Mech. **94**(10), 793–817 (2014)
6. Després, B., Poëtte, G., Lucor, D.: Robust uncertainty propagation in systems of conservation laws with the entropy closure method. In: Uncertainty Quantification in Computational Fluid Dynamics, pp. 105–149. Springer (2013)
7. Fisher, P., Tate, N.: Causes and consequences of error in digitalk elevation models. Prog. Phys. Geogr. **30**(4), 467–489 (2006)
8. Fjordholm, U.S., Mishra, S., Tadmor, E.: Well-balanced and energy stable schemes for the shallow water equations with discontinuous topography. J. Comput. Phys. **230**(14), 5587–5609 (2011)
9. Ge, L., Cheung, K., Kobayashi, M.: Stochastic solution for uncertainty propagation in nonlinear shallow-water equations. J. Hydraul. Eng. **134**(12), 1732–1743 (2008)
10. Ghanem, R., Spanos, P.: Stochastic Finite Elements: A Spectral Approach. Springer, New York (1991)
11. Godunov, S.: Finite difference schemes for numerical computation of solutions of the equations of fluid dynamics. Math. USSR Sb. **47**, 271–306 (1959)
12. Gosse, L.: A well-balanced flux-vector splitting scheme designed for hyperbolic systems of conservation laws with source terms. Comput. Math. Appl. **39**(9–10), 135–159 (2000)
13. Gosse, L., Leroux, A.-Y.: a well-balanced scheme designed for inhomogeneous scalar conservation laws. Comptes Rendus De L Academie Des Sciences Serie I-mathematique **323**(5), 543–546 (1996)
14. Greenberg, J.M., Leroux, A.-Y.: A well-balanced scheme for the numerical processing of source terms in hyperbolic equations. SIAM J. Numer. Anal. **33**(1), 1–16 (1996)
15. Jin, S.: A steady-state capturing method for hyperbolic systems with geometrical source terms. ESAIM. Math. Model. Numer. Anal. **35**(04), 631–645 (2001)

16. LeVeque, R.J.: Balancing source terms and flux gradients in high-resolution Godunov methods: the quasi-steady wave-propagation algorithm. J. Comput. Phys. **146**(1), 346–365 (1998)
17. Liu, D.: Uncertainty Quantifications with Shallow Water Equations. Ph.D. thesis, TU Braunschweig and University of Florence (2009)
18. Mishra, S., Schwab, C., Sukys, J.: Multi-level monte carlo finite volume methods for shallow water equations with uncertain topography in multi-dimensions. In: Technical Report 2011-70, Seminar for Applied Mathematics. ETH Zürich, Switzerland (2011)
19. Perthame, B., Simeoni, C.: Convergence of the upwind interface source method for hyperbolic conservation laws. In: Hyperbolic Problems: Theory, Numerics, Applications, pp. 61–78. Springer (2003)
20. Poëtte, G., Després, B., Lucor, D.: Uncertainty quantification for systems of conservation laws. J. Comput. Phys. **228**(7), 2443–2467 (2009)
21. Roe, P.L.: Approximate riemann solvers, parameter vectors, and difference schemes. J. Comput. Phys. **43**(2), 357–372 (1981)
22. Roe, P.L.: Upwind differenced schemes for hyperbolic conservation laws with source terms. In: Proceedings of the Conference Hyperbolic Problems, pp. 41–51 (1986)
23. Tryoen, J., Matre, O.L., Ern, A.: Adaptive anisotropic spectral stochastic methods for uncertain scalar conservation laws. SIAM J. Sci. Comput. **34**(5), A2459–A2481 (2012)
24. Vázquez-Cendón, M.E.: Improved treatment of source terms in upwind schemes for the shallow water equations in channels with irregular geometry. J. Comput. Phys. **148**(2), 497–526 (1999)
25. Xing, Y., Shu, C.-W.: High order well-balanced finite volume weno schemes and discontinuous galerkin methods for a class of hyperbolic systems with source terms. J. Comput. Phys. **214**(2), 567–598 (2006)
26. Xiu, D.: Numerical Methods for Stochastic Computations. Princeton Univeristy Press, Princeton (2010)
27. Xiu, D., Karniadakis, G.: The Wiener–Askey polynomial chaos for stochastic differential equations. SIAM J. Sci. Comput. **24**(2), 619–644 (2002)
28. Xiu, D., Shen, J.: Efficient stochastic galerkin methods for random diffusion equations. J. Comput. Phys. **228**(2), 266–281 (2009)